The effects of greening a parking lot as a heat mitigation strategy on outdoor thermal stress using fixed and mobile measurements: case-study project “tertiary forest”

Sophie Parison, Maxime Chaumont, Raphaëlle Kounkou-Arnaud, Frédéric Long, Andrej Bernik, Marcos da Silva, Martin Hendel

The Effects of Greening a Parking Lot as a Heat Mitigation Strategy on Outdoor Thermal Stress Using Fixed and Mobile Measurements: Case-Study Project "Tertiary Forest"

Sophie Parison[*1¶], Maxime Chaumont[1¶], Raphaëlle Kounkou-Arnaud[2], Frédéric Long[2], Andrej Bernik[3], Marcos Da Silva[3], Martin Hendel[1,4]

[¶] *These authors contributed equally to this work.*
**corresponding author: sophie.parison@u-paris.fr*

[1] Université Paris Cité, LIED, UMR 8236, CNRS, F-75013, Paris, France
[2] Météo-France, Direction des Services Météorologiques, Saint-Mandé, France
[3] Fieldwork Architecture, F-75020, Paris, France
[4] Univ Gustave Eiffel, ESIEE Paris, département SEED, F-93162 Noisy-le-Grand, France

Abstract: An asphalt-concrete parking lot was converted to a small urban forest with 72 trees and permeable pavement as an urban heat island countermeasure. Microclimate monitoring was performed pre- and post-renovation using fixed and mobile measurements. We propose a protocol to estimate robust statistical effects over 24h constructed with several days of observation, and to compare the spatial distribution of heat stress pre- and post-conversion regardless of differences in weather conditions. Detailed effects on solar and infrared radiation, microclimate and pedestrian heat stress are assessed and tested for statistical significance. Great improvements of pedestrian heat stress are reported, especially in daytime, following the creation of shade which significantly reduces the radiative load of the area. *UTCI*-equivalent temperature is reduced up to 6.2°C (3.1°C on a 24h-average). Mobile measurements were used to characterize the spatial disparity of heat stress. Strong thermal discomfort is exhibited under direct insolation. At night, positive effects on pedestrian heat stress are slightly counterbalanced by an increase in infrared trapping due to the reduction of the sky view factor beneath the trees while wind speed is slowed. Recommendations are formulated for urban planners.

Keywords: heat mitigation, urban heat island, urban cooling, urban greening and vegetation, thermal comfort, mobile/fixed microclimatic measurements.

Highlights

- Microclimatic effects of greening is assessed with fixed/mobile measurements.
- The protocol is suited regardless of differences in weather between observations.
- Heat stress pre- and post-renovation shows great spatial heterogeneities.
- Trees have strong impacts on the radiative load, microclimate and heat stress.
- Vegetation reduces wind speed and slightly increases infrared trapping at night.

Notations

AH	absolute humidity [g/m^3]
L	incident (downwards) infrared radiation (3 - 100 µm) [W/m^2]
L_{up}	upwards infrared radiation (3 - 100 µm) [W/m^2]
S	incident (downwards) solar radiation (0.3 -3 µm) [W/m^2]
S_{up}	reflected (upwards) solar radiation (0.3 -3 µm) [W/m^2]
T_a	air temperature [°C]

$T_a^{control}$	air temperature at control site [°C]
T_g	black-globe temperature [°C]
H/W	canyon aspect ratio
MRT	mean radiant temperature [°C]
$MRT - T_a$	radiative load [°C]
PET	Physiological Equivalent Temperature [°C]
RH	relative humidity [%]
SVF	sky view factor
stat. sign.	statistically significant
UHI	urban heat island
$UTCI$	Universal-Thermal-Climate-Index-equivalent temperature [°C]
$\Delta UTCI$	thermal "over-stress" : relative stress compared to a shaded area

1. Introduction

In the past century, rural-to-urban migration has gradually increased until it reached the threshold of more than half of the world population living in urbanized areas in 2016 (Vardoulakis & Kinney 2019). In the past decades, the growing number of urban dwellers along with the rise in population has led to rapid urbanization of the land. Urban areas present high densities of inhabitants, artificial surfaces, and scarcity of vegetation (Santamouris et al. 2015). These features primarily met for needs for practicality and walkability within cities. However, the higher share of used land has come with human-induced negative effects on environment, such as soil, water and air quality degradation or depletion of biodiversity (IPCC 2019). At local scale, urban sprawl also modifies wind patterns, increase energy consumption and create or amplify existing urban heat islands (*UHI*) (Uttara et al. 2012). Concomitantly, climate change exacerbates this stresses and increases health risks and vulnerability (Mitchell et al. 2016, Garschagen & Romero-Lankao 2015, Li et al. 2012). As a consequence, cities seek for guidelines for adapting urban planning policies in order to tackle these aspects. One major topic is that of heat mitigation to limit impacts on health and improve thermal comfort of the population in densely-built areas.

A variety of urban cooling strategies exist, which usually act on one or several specific aspects of the energy balance of the city's lower atmosphere (Oke 1982). For instance, cool urban materials counterbalance the negative impacts of dark impervious surfaces with a higher reflectivity/emissivity, modified thermal inertia or with pervious/green alternative surfaces (Nwakaire et al. 2020, Parison et al. 2020a, Parison et al. 2021). Energy efficiency methods can also be promoted, while the use of watering cooling techniques as well as greening techniques make up for the lack of vegetation in urban areas in general (Hendel et al. 2016, Santamouris 2015). Among heat mitigation strategies, urban greening is undoubtedly one of the best-known and most efficient existing passive solution for cooling the urban microclimate (Li et al. 2022, Hiemstra et al. 2017, Akbari et al. 2001). In addition, urban greening also presents a huge number of co-benefits, such as improving the air and soil quality (Setälä et al. 2013), increasing local attractiveness and perceived quality of life (Sheets & Manzer 1991), and helping preserve biodiversity (Pena et al. 2017, Shuaib et al. 2018).

Urban vegetation thus plays a substantial role on the improvement of outdoor thermal comfort, principally thanks to the shade and evapotranspiration it provides (Das et al. 2022, Zheng et al. 2021). Many studies have investigated the effects of trees, grass, parks, green roofs or façades on microclimate and thermal comfort. Kong et al. (2017) summarized and compared results of 21 studies (simulations and measurements) regarding the effects of trees. They report reductions of solar radiation (80 - 95%), air temperature (-1 to 2°C on average), mean radiant temperature (*MRT*) (-2° to -47°C, and -5.1°C on average at pedestrian height), wind speed (15% - 80%), and

Physiological Equivalent Temperature (*PET*) (-2 to -20°C), despite a reported increase of relative humidity (+5 to +31%). Overall, vegetation strongly reduces *MRT* following the creation of shade, leading to reduced heat stress (up to a few degrees on average), with small reductions of air temperature and negligible increase of relative humidity (Jia & Wang 2021, Teshnehdel et al. 2020, Coccolo et al. 2018). The combined effect of tree layout and urban morphology on microclimate was also largely investigated, with the goal of orienting urban planners in green designs (Mahmoud & Abdallah 2022, Azcarate et al. 2021, Abdi et al. 2020). Raman et al. (2021a) showed that wind-sheltered zones were high heat-stress areas and hence best beneficiaries to tree planting. Improvement of thermal comfort daytime is strongly dependent on foliage density (shade percentage), while other parameter such as height, planting density and layout with regard to wind patterns also plays a role (Raman et al. 2021b, Morakinyo et al. 2017).

In order to assess the conversion's impact on microclimatic parameters, fixed measurements can be deployed for the evaluation of thermal comfort in the built environment with adequate microclimatic monitoring (Shashua-Bar et al. 2011, Van Hove et al. 2015, Wang & Akbari 2016). However, most of the time experimental studies are conducted after construction (Fu et al. 2022, Bowler et al. 2010, Takebayashi & Moriyama 2009). Indeed, identifying sites early enough to prepare a measurement campaign before and after transformation can be challenging, hence meteorological monitoring ahead of construction works is rare. Thus, most of the time such studies evaluate the current situation of the site without taking interest in the impact of the transformation of the area between pre- and post-states. Simulations however, usually facilitate this task (Milošević et al. 2017, Kong et al. 2017), with relevant greening performance indicators from an adequate assessment toolbox (Bouzouidja et al. 2021a).

Fixed measurements, when associated with a proper statistical procedure, allow for precise and robust estimation of the average impact of a site's transformation, as demonstrated in previous work (Parison et al. 2020b), but require heavy and permanent instrumentation for a long period of time. For this reason, in order to spatially mesh microclimate parameters in several areas with moderate constraints and costs, mobile measurements are often preferred over large networks, as they require less instrumentation (Leconte et al. 2015, Shi et al. 2018, Pigliautile & Pisello 2018, Qi et al. 2021 & 2022, Sulzer et al. 2022). However, because fewer data samples are collected, mobile measurements are usually less robust than fixed measurements. While the latter allow for characterization of a complete day, the former focuses on a specific narrow time window during each mobile measurement campaign. Both approaches can be also be combined (Parece et al. 2016).

In this paper, we propose a comprehensive approach combining both measurement methods for various microclimatic parameters. The method is applied on a case-study project named "Tiertiary Forest", which converted a parking lot in the Paris Metropolitan Area (France) into a small urban forest with permeable concrete. This project and its construction schedule offered an opportunity to study the site before and after greening. To this aim, microclimatic measurements were conducted to determine the transformation's cooling effects. The goal of this paper is to propose a comprehensive methodology for assessing the microclimatic effects of an urban site's transformation, and to apply it on a the case-study site to improve knowledge about urban greening on outdoor thermal comfort during the summer. Both methodological and assessment goals were set. Specifically, the following research angles were addressed:

Fixed measurements:

- Estimate the effects over 24h statistically, combining measurements pre- and post-conversion regardless of weather conditions
- Characterize the cooling impacts of the site's conversion where the most trees were planted, with emphasis on pedestrian heat stress and radiation

Mobile measurements:

- Compare pre- and post-conversion states regardless of temporal drift and differences in weather conditions
- Evaluate the spatial distribution of heat stress over several areas of the site at different stages of the project

This paper presents results following the conversion of the site, i.e. after trees were planted and permeable concrete was laid. The conversion's impact on pedestrian heat stress is assessed using a statistical procedure, allowing for robust estimation of the effects during an average 24-h radiative summer day. In particular, effects are characterized for: solar and infrared radiation (incident and upwards), wind speed and wind direction, air temperature, relative and absolute humidity, radiative load, and heat stress (using *UTCI*). In addition, mobile measurements are used for spatial characterization of the site. A reference point is used to compare *UTCI* temperatures from mobile measurements gathered and compared at different stages of the project.

2. Materials and Methods

2.1. Site Description

The site chosen for the study is a privately-owned parking lot of about 1,200 m² for the occupants of a home for young workers in the municipality of Aubervilliers, located North of Paris (France). The conversion is part of a multidisciplinary project called "Tertiary Forest", involving climate and environmental scientists, architects and urban planners as well as local officials (Fieldwork 2023). The project aims to transform the parking lot into a small urban forest, and is driven by the desire to mitigate heat and create a more pleasant outdoor space for the residents. Conversion of the parking lot took advantage of a newly built metro line close by, which permitted reducing the number of parking spaces.

The site is located in a heterogeneous urban area surrounded by tall buildings. It can be classified as LCZ 4 (open high-rise), with adjacent constructed areas falling under LCZ 2 (compact mid-rise) and a neighboring 2.5 ha park (LCZ B, scattered trees) to the North (Stewart and Oke, 2012) (see Figure 3). Prior to renovation, the site offered no amenities for pedestrians, such as benches, shade or footpaths. It offered little to no vegetation apart from peripheral flowerbeds and sparsely-planted trees. The ground was paved with old impervious asphalt concrete with an albedo of 0.13 as measured per ASTM E1918-16 (ASTM 2016). Photographs of the area in its initial state are shown in Figure 1.

Considering the initial site's characteristics, it was a good candidate for conversion to a green area for heat mitigation. The site was completely redesigned into a pedestrian-friendly space for residents with benches, no longer accessible to vehicles. A total of 72 trees were planted with a higher density in the sunniest areas, creating a "tertiary forest". Trees were not planted into individual pits (as often done in urban spaces) to favor mycorrhization and connections between roots. The top asphalt concrete layer was entirely replaced with permeable concrete with an albedo of 0.24, and a passive underground water storage system collects rainwater. The permeability and water storage aim to improve soil fertility, vegetation health and growth. Although not replaced during conversion, the soil was also enriched with compost. Photographs of the area post renovation (2020) are provided in Figure 2.

The project and its schedule offered a unique opportunity to monitor the site ahead of initial demolition works. Microclimatic measurements were conducted before and after renovation with two fixed weather stations installed by Météo-France. The case station is placed in the parking lot in an area where numerous trees were planted, while the control station is located on a rooftop approximately 30 meters above the parking lot, outside of the project's area of influence. Figure 3 shows the fixed weather stations' positions and the project's conversion plan.

Figure 1: Photographs of the site before conversion in 2017.

Figure 2: Photographs of the site after conversion in 2020 and 2021.

Table 1: Main characteristics of the site.

Studied area	1200 m², with surrounding LCZ 4, 2 and B
Before conversion	
Pavement	Impervious asphalt concrete (albedo: 0.13)
SVF	0.7 (at case station location)
After conversion	
Pavement	Pervious concrete (albedo 0.24, porosity: 15%, drainability: 50L/m²/s)
SVF	0.2 (at case station location)
Vegetation	72 trees covering 380 m²
Tree species	*Acer campestre* (maple), *Quercus ilex* (oak), *Ulmus resista* (elm)
Plantation specificities	4-m-high trees when planted Unsealed roots in bare soil for mycorrhiza development
Water collection	Passive underground rainwater storage (infiltration) Run-off to trees via natural gradient

The sky view factor (*SVF*) was estimated using SAGA GIS modelling (function *Potential Incoming Solar Radiation*) (see Hendel et al. 2020) at the case station location at a value of 0.7 before and 0.2 after greening. Table 1 summarizes the main characteristics of the site.

The first measurements were performed during the summer of 2018 prior to demolition, while trees were planted and most of the asphalt concrete was removed after partial conversion in 2019 (with permeable concrete below the case station area while most of the rest remained bare, unsealed soil). Construction works were fully completed for the 2020 measurement campaign.

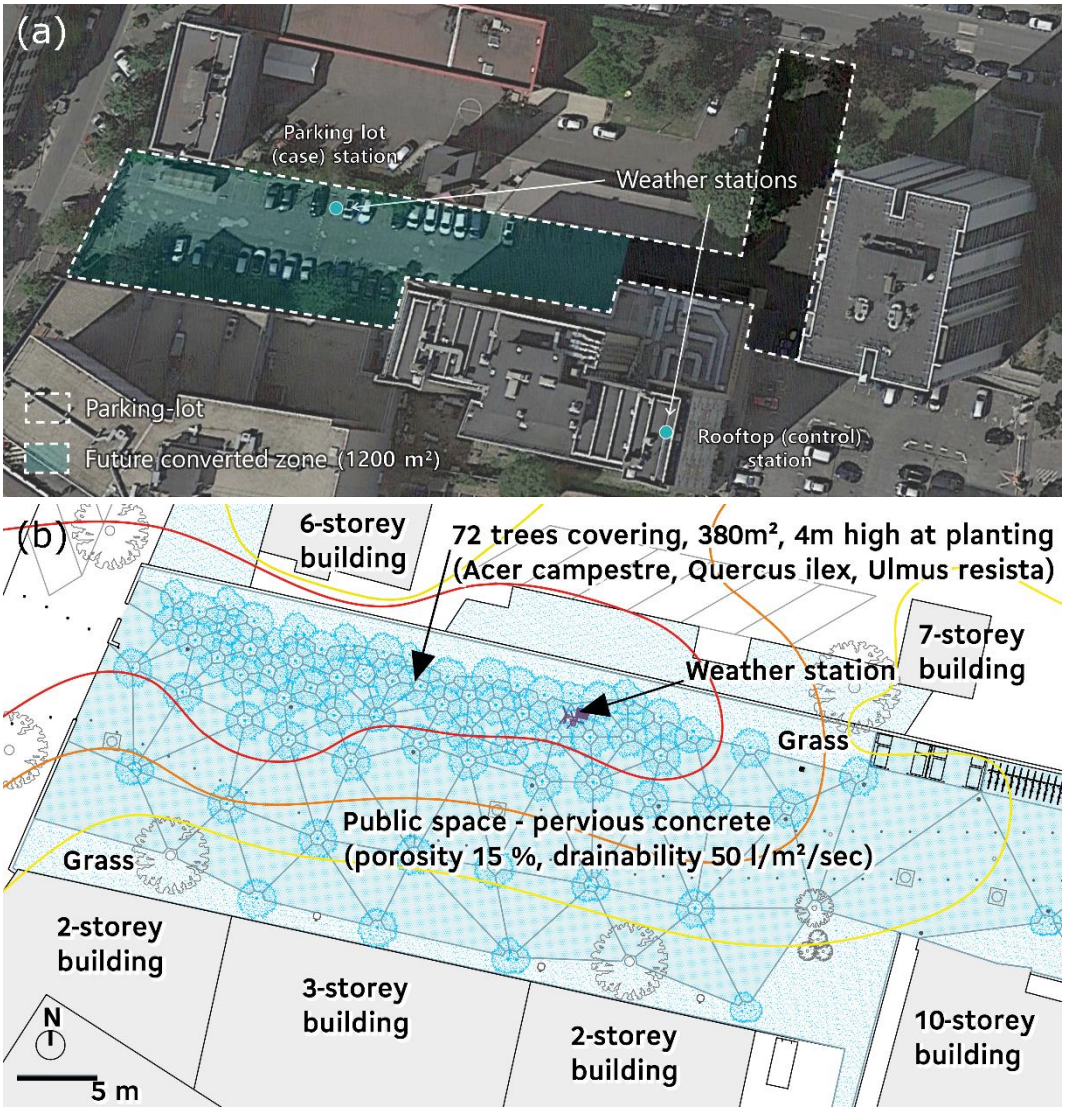

Figure 3: Site map before conversion and weather station positions (a), and project plan (b). The case station is located in the parking lot, while the control station is located on a rooftop.

2.2. Instrumentation

The weather stations monitor several microclimatic parameters continuously every minute at screen height: air temperature, relative humidity, black globe temperature and wind speed, in addition to long and shortwave upward and downward radiation fluxes, as well as a rain gauge near the control (rooftop) station. In addition to the fixed station measurements, mobile microclimatic measurements were also conducted in order to characterize the site's heat stress spatial variability. A photograph of the fixed and mobile weather stations is shown in Figure 4.

Table 2 lists the instrument characteristics used for the fixed weather stations, while Table 3 lists that of the mobile weather station. Note that for the control rooftop station, the instrument height is about 30 meters higher than the ground level.

Figure 4: Rooftop (left) and parking lot (center) fixed weather stations, and mobile (right) weather station (before conversion of the site).

Table 2: Instrument type, measurement height and accuracy for the two fixed weather stations.

Fixed weather stations

Parameter	Instrument and manufacturer	Height	Accuracy
Air temperature	Sheltered Pt100 (Guilcor)	1.6 m	± 0.3°C
Relative humidity	Sheltered capacitive hygrometer (HMP110, Vaisala)	1.6 m	± 1.5%
Black-globe temperature	Pt100 - ISO 7726 (Campbell Sci)	1 m	± 0.2°C
Wind speed and direction	Propeller wind monitor (5103, Young)	1.8 m	± 3° ± 0.3m/s
Radiation (solar/infrared)	Four component net radiometer (CNR1, Kipp and Zonen)	0.6 m	± 2.5%
Air pressure	Digital barometer (PTB210, Vaisala)	0.5 m	± 0.3 hPa
Pluviometry	Rain gauge (3039, Precis Mécanique)	0.8 m	± 5%

Table 3: Instrument type, measurement height and accuracy for the mobile weather station.

Mobile weather station

Parameter	Instrument and manufacturer	Height	Accuracy
Air temperature	Sheltered Pt 100 (DMA672, LSI-Lastem)	1.5 m	± 0.1°C
Relative humidity	Sheltered capacitive hygrometer (DMA672, LSI-Lastem)	1.5 m	± 1.5%
Black-globe temperature	Pt100 - ISO 7726 (EST131, LSI-Lastem)	1.5 m	± 0.15°C
Wind speed (v)	Hot-wire anemometer (ESV107, LSI-Lastem)	1.5 m	± (0.05+0.05v) m/s

2.3. Data Treatment Procedure

○ Fixed Microclimatic Measurements

The protocol we propose estimates the impact of the site's transformation each minute over 24h, for an average summer day constructed from several observation days before and after conversion, regardless of the differences in weather conditions between days. The statistical test (fixed-effects model) (described by Parison et al. (2020b)) uses a "Before-After-Control-Impact" (BACI) configuration, which requires sampling data both before and after transformation of the site at adequate case and control locations (Stewart-Oaten & Murdoch, 1986).

Assessment of the impact (for a given microclimatic parameter) is achieved by testing whether the interstation profile, i.e. the difference measured between case (parking lot) and control (rooftop) stations, changes once the transformation of the site is completed. This allows us to extract the impact of the transformation regardless of weather conditions and regardless of pre-existing differences between case and control stations, i.e. prior to the site's transformation. This is valid as long as the control remains unchanged after transformation. Here, the interstation profile at time t is monitored during two periods: before (in 2018) and after (in 2020 and 2021) site conversion.

Only radiative days are considered for the analysis, occurring from June 1st to August 31st. They must present anticyclonic weather conditions: clear skies (<3 oktas), low wind speeds (< 3m/s), and no rain. Radiative days preserve the small-scale modifying effects of the surface (Kousis et al. 2022). For this study, 13 days meet the criteria for radiative days in 2018 (before conversion) against 19 days in both 2020 and 2021 (after conversion).

Noting M the measured meteorological parameter of interest, the average impact $\underline{I}$ of the conversion of the site on M is obtained by considering the difference between: *i)*-the interstation profile after conversion of the site, denoted $\underline{\Delta M_{after}}$, and averaged over n_{after} radiative days (here, n_{after}= 19 days), and *ii)*-the interstation profile before conversion, denoted $\underline{\Delta M_{before}}$, averaged over n_{before} radiative days (here, n_{before}= 13 days). This procedure is summarized in Equation (1):

$$\underline{I} = \underline{\Delta M_{after}} - \underline{\Delta M_{before}}$$
$$= \frac{1}{n_{after}}\left(\sum_{i=1}^{n_{after}} M^i_{case}(t) - M^i_{control}(t)\right) - \frac{1}{n_{before}}\left(\sum_{i=1}^{n_{before}} M^i_{case}(t) - M^i_{control}(t)\right) \quad (1)$$

The null hypothesis is that of a non-existent average impact ($\underline{I} = 0$), which is then tested for statistical significance with a confidence interval of 95%. Observations are statistically significant (stat. sign.) if the null hypothesis is rejected, i.e. observations are outside of the margin of error. Otherwise, results are not stat. sign. (within the margin of error). The impact $\underline{I}$ is estimated for each sampled minute, meaning that a total of 1440 statistical tests are performed in order to isolate the average effects of the site's conversion on a whole day.

Figure 5 shows an example of meteorological data measured at the case station during radiative days (valid for procedure): global downwards and upwards solar radiation (resp. S and S_{up}) as well as downwards and upwards infrared radiation (resp. L and L_{up}) are shown for June 26th, 2018 before transformation (lefthand figure) and for June 14th, 2021 after transformation (righthand figure). The corresponding control station measurements are shown in the embedded upper-right corner plot. As seen, solar irradiance as well as other fluxes are greatly altered after conversion of the site with regard to the unaltered control station. The difference between periods (before/after) of the case-control difference allows us to statistically quantify this impact in the results section combining several days, following the procedure described above.

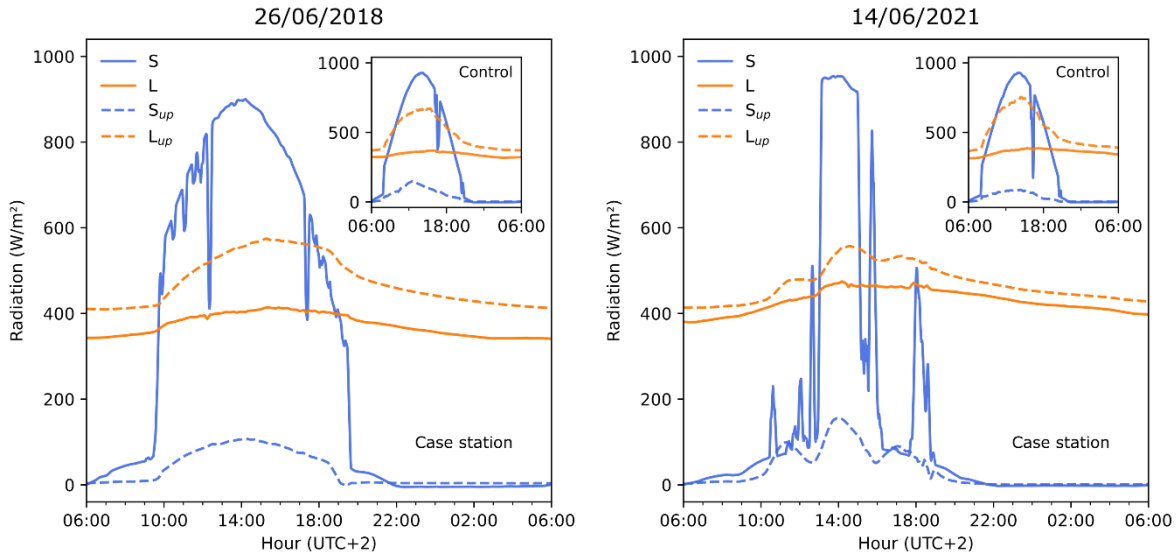

Figure 5: Example of radiation for radiative days before (26/06/2018) and after (14/06/2021) conversion: global incident (S) and upwards (S_{up}) solar radiation (blue lines), and incident (L) and upwards (L_{up}) infrared radiation (orange lines), measured at the case (parking lot) station. The upper-right corner plots represent the same parameters measured simultaneously for the control (rooftop) station.

- **Mobile Measurements**

In addition, mobile measurements were performed in order to study the spatial distribution of microclimatic conditions on site. While mobile measurements can capture spatial variations, they cannot capture temporal variations outside of the duration of a mobile measurement campaign, unlike fixed weather station measurements.

Stop-and-go mobile measurements were conducted twice, before conversion on June 26th 2018 and after conversion on September 9th 2021. Transects were performed on radiative days (anticyclonic conditions), following recommendations on optimized mobile measurement procedure regarding instrumentation stabilization time of ten to twenty minutes (Qi et al. 2021).

From these measurements, the Universal Thermal Climate Index (*UTCI*)-equivalent temperature was calculated (Fiala et al. 2012). Mobile measurements are compared to a reference (noted ref) stress level to account for weather differences between measurement campaigns conducted years apart. This reference level corresponds to a theoretical permanently-shaded sheltered courtyard where air temperature and relative humidity are those measured at the control (rooftop) station, while wind speed is assumed to be 0.5 m/s at a height of 1.5 m and mean radiant temperature (*MRT*) is assumed equal to the control air temperature (as for a heavily shaded area). The difference between the calculated *UTCI* at a given point of the sites and the reference *UTCI* at the same time allows us to estimate the over- or under-heating of the study point with regard to the reference *UTCI* at the same moment. This indicator, calculated using Equation (2), is hereafter referred to as "thermal over-stress" and denoted $\Delta UTCI$.

$$\Delta UTCI = UTCI^{mobile} - UTCI^{ref}(T_a^{control}, RH^{control}, MRT^{ref} = T_a^{control}, v^{ref} = 0.5\ m/s) \quad (2)$$

This methodology is used by Karam et al. (2022) to compare mobile data from different measurement campaigns in order to quantify the microclimatic effects of a site's transformation. Similarly, in the literature, some studies propose a control protocol to compare measurements within a campaign. For example, Leconte et al. (2015) compared the temporal mean of control areas to the spatial mean of the measurement points. For their part, Pigliautile & Pisello (2018) repeated the same routes in different orders each time, though multiple methods exist (Kousis et al. 2022, Xiong et al. 2022, Peng et al. 2022, Vasilikou & Nikolopoulou 2020).

○ **Summary of the measurement periods and parameters studied**

Table 4 summarizes the chronology of the measurements performed from 2018 to 2021 during summer periods (1st June to 30th Sept.).

Table 4: Chronology of the measurements performed each summer (from 1st June to 30th Sept.).

Before conversion (summer of 2018)
• Continuous fixed measurements at case and control sites (13 radiative days) • Mobile measurements on June, 26th from 2:30 pm to 5:30 pm (UTC+2)
After conversion (summer of 2020 and 2021)
• Continuous fixed measurements at case and control sites (19 radiative days) • Mobile measurements on Sept., 9th from 2:30 pm to 5:30 pm (UTC+2)

Results are presented on four radiative components (solar/infrared, incident/upwards), wind speed and direction, air temperature (T_a), relative (RH) and absolute humidity (AH), radiative load ($MRT-T_a$) and $UTCI$-equivalent temperature. Indeed, AH is independent from T_a contrary to RH. Similarly, radiative load ($MRT - T_a$) is an independent variable contrary to MRT.

3. Results and Discussion

3.1. Fixed Microclimatic and Radiative Measurements

We now present the average effects (Eq. 1) of the site's conversion. Those effects are representative of the impact of the conversion at the case station position (see Figure 3). For each graph, assessment is based on 13 observation days before and 19 after renovation. Prior to the analysis, raw data is smoothed with a ten-minute moving average and data is filtered for radiative days. Upcoming results are given in local time (UTC+2).

○ **Average Effects on Radiation**

The effects on the four radiative components measured 60 cm above ground level are shown in Figure 6 (downward S and upward S_{up} solar radiation, and downward L and upward L_{up} infrared radiation).

The blue envelope represents the margin of error of the statistical test with a 95% confidence interval outside of which effects are statistically significant. The blue curve shows the average impact of conversion for each minute of the day. The average value of the statistically significant effects, their duration (in hours per day, rounded to the nearest 5-minute step) and the value of the maximum stat. sign. effects are summarized in Table 5. To further account for the robustness of the effects (both in amplitude and duration), a single statistical test is also performed on the whole dataset averaged over 24h. The 24h-average value as well as the associated p-value are reported in Table 5.

Table 5: Mean, maximum and duration of the statistically significant effects of the site's conversion on radiation at case station location, 24h-average effect and associated p-value if statistically significant.

	Solar radiation		**Infrared radiation**	
	S	***S_{up}***	***L***	***L_{up}***
Average value of the stat. sign. events (W/m²)	-222	+28	+43	-24
Duration of the stat. sign. events	10h40m	12h	24h	18h20m
Maximum stat. sign. effect (W/m²)	-561	+85	+54	-67
24h-averaged value (W/m²)	-102	+13	+43	-20
p-value associated with the 24-h average if stat. sign.	1.1e-9	1.0e-9	2.9e-9	4.1e-7

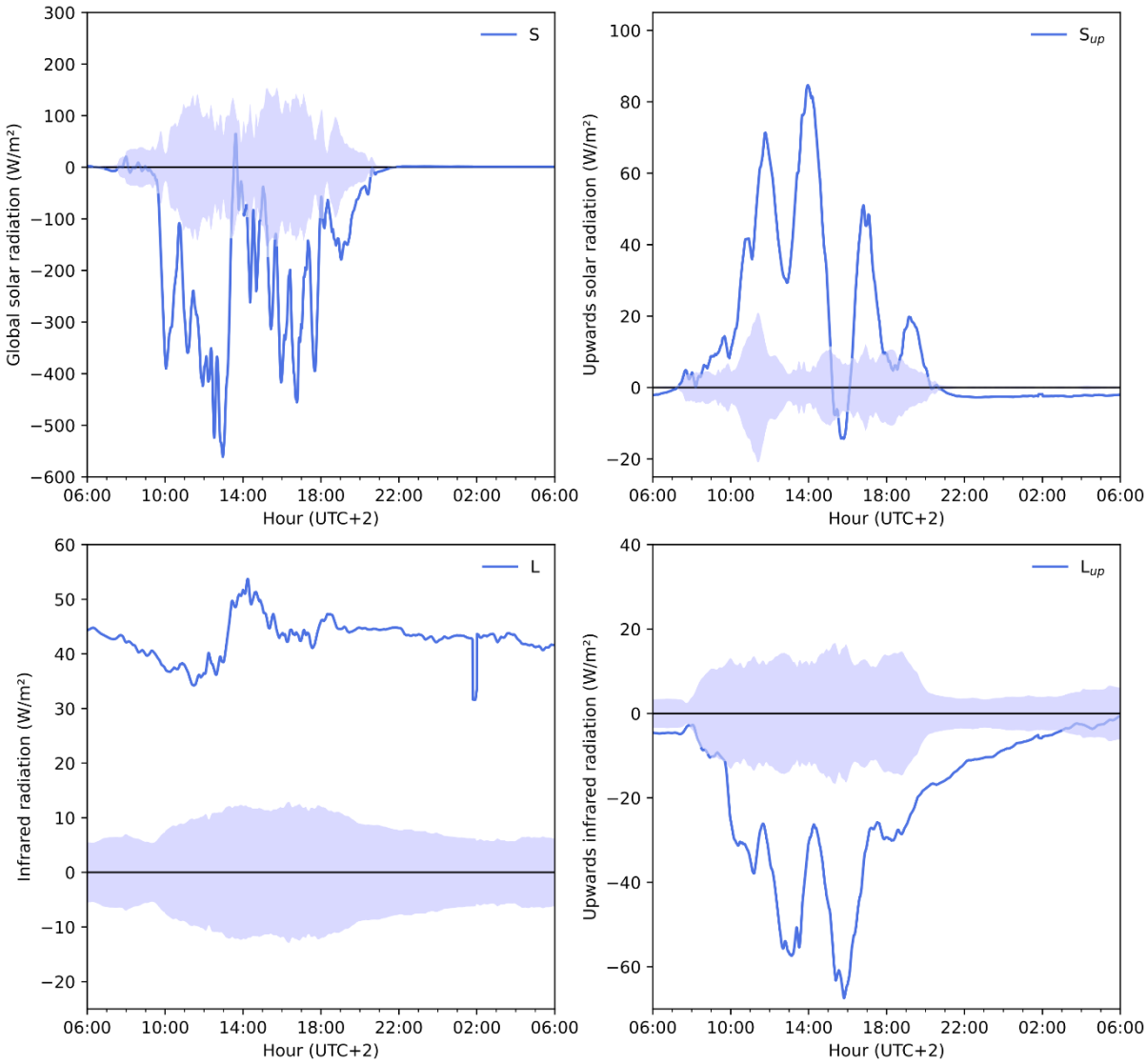

Figure 6: Average radiative effects of the site's conversion. (S): Solar incident radiation, (S_{up}): upwards solar radiation, (L): infrared incident radiation, (L_{up}): upwards infrared radiation. The filled area is the margin of error with a 95% confidence interval, outside of which average effects (blue curve) are statistically significant (assessment based on 13 observation days before and 19 after renovation).

As we can see, the impact of the transformation of the parking lot is quite significant. Looking at the details, it is clear from the observations that the shade provided by the trees planted in the immediate vicinity of the weather station as well as repaving of the area have a very strong, robust and long lasting impact on radiation throughout the day.

Shading provided by the trees causes a strong reduction of the incident solar radiation S, up to 561 W/m² around 1pm and by 222 W/m² on average. Reduction of S is stat. sign. more than 10 hours per day (almost all of the insolation period). Also, as a result of replacing the asphalt concrete with an albedo of 0.13 with permeable concrete with an albedo of 0.24, reflected solar radiation S_{up} increases up to 85 W/m² and by 28 W/m² on average, despite the significant decrease of solar irradiance. Those effects are stat. sign. about 12 hours per day. Effects on solar radiation appear stronger in the morning and early afternoon, from 10am to 1pm approximately, as well as in the afternoon, roughly from 3:30pm to about 6:30pm depending on the parameter. This is likely correlated to the shading pattern offered by the planted trees.

Incident infrared radiation L is found to marginally increase after conversion of the site, by a relatively stable average of 43 W/m² with limited fluctuations. Most notably, the effect is always

statistically significant throughout the 24h-day. This is likely due to the cover now offered by the surrounding trees, which reduces the sky view factor (from 0.7 to 0.2) and thus mitigates radiative cooling. Finally, the upwards infrared radiation L_{up} is found to decrease, especially during the day (up to 67 W/m²) and by 24 W/m² on average during more than 18 hours. Upwards longwave radiation can either be reflected by the ground or directly emitted by thermal radiation. Given the high emissivity of standard pavement materials, the former mechanism usually represents a small proportion of L_{up} as compared to that of the latter. Therefore, the increase in L_{up} is most likely the result of the reduction of the pavement's temperature thanks to shading and higher albedo compared to the previous asphalt-concrete surface, as confirmed in similar studies (Bouzouidja et al. 2021b). As seen, although greater during the day, effects on L_{up} last until 3am the next day.

For both S_{up} and L_{up}, positions of the peaks roughly match those observed for incident solar radiation S which drives the behaviors observed for both of these parameters. All effects on radiation are extremely robust, as 24-h average tests all yield stat. sign. results (see Table 5), which indicate both strong and long-lasting effects.

Future tree growth will provide longer-lasting, more substantial shading that is likely to further reduce incident solar radiation (S), while reflected solar radiation (S_{up}) underneath the trees should decrease, as less ground surface will be directly exposed to insolation. Further reduction of the sky view factor should further increase incident infrared radiation (L), while upwards infrared (L_{up}) should arguably decrease as well, at least during the day while it is more debatable at night. While reductions of incident solar radiation S and upwards infrared radiation L_{up} should be beneficial to mitigate pedestrian heat stress, the increase of reflected solar radiation S_{up} as well as that of downwards infrared radiation L could lead to potential drawbacks, all else being equal.

- **Average Microclimatic Effects**

The microclimatic impacts of the site's conversion following the removal of the asphalt concrete pavement and the planting of trees are reported in Table 6, for air temperature, relative humidity and radiative load ($MRT - T_a$) as well as their combined impact on *UTCI*-equivalent temperature. Contrary to radiation, effects are representative of pedestrian height (between 1 m and 1.8 m depending on the parameter, see Table 2).

Table 6: Mean, maximum and duration of the statistically significant microclimatic effects of the site's conversion at case station location, 24h-average effect and associated p-value if statistically significant.

	T_a	RH	$MRT-T_a$	$UTCI$
Average value of the stat. sign. events	-0.5°C	+1.6%	-8.2°C	-3.1°C
Duration of the stat. sign. events	15h20m	5h40m	19h35m	11h10m
Maximum stat. sign. effect	-1.3°C	+2.3%	-27°C	-6.2°C
24h-averaged value	-0.3°C	Not stat. sign.	-7.5°C	-1.4°C
p-value associated with the 24-h average if stat. sign	2.0e-4	Not stat. sign.	1.4e-13	5.9e-4

As for the effects on radiative fluxes, the microclimatic impact of the site's transformation is substantial. Globally, effects are extremely robust, with 24-h average tests yielding stat. sign. results (Table 6), with an exception for relative humidity. We start with the effects on air temperature and relative humidity, illustrated in Figure 7.

*

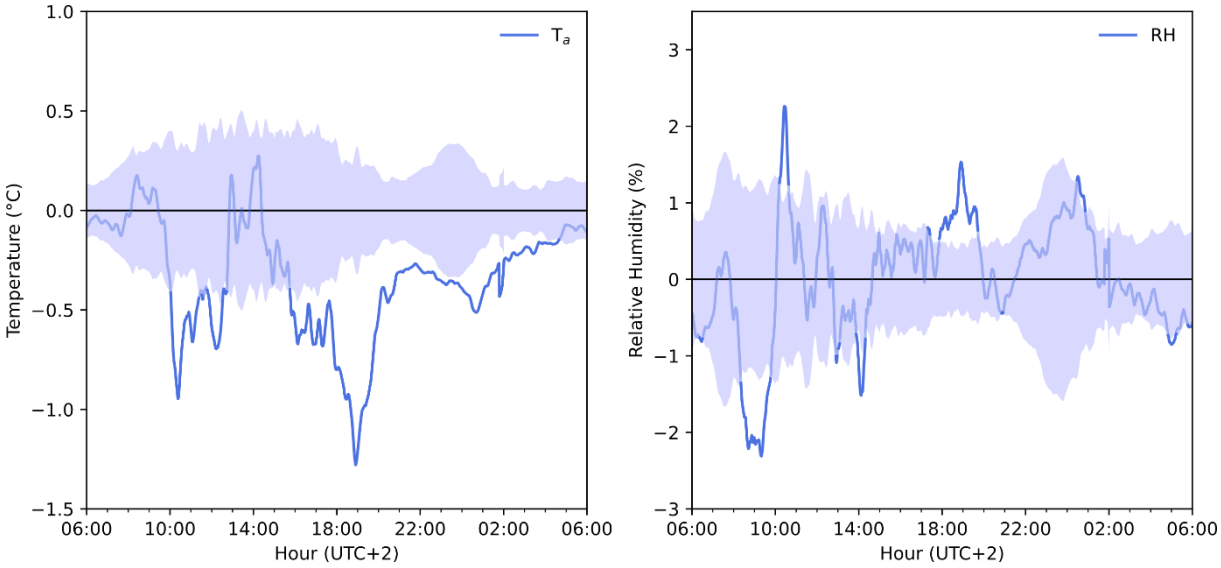

Figure 7: Average microclimatic effects of the site's conversion. (T_a): air temperature, (RH): relative humidity.

Air temperature is significantly reduced all day starting from 10 am to 5 am the next day, with an interruption between 12:30 and 3:30 pm, which coincides with the increase in solar radiation observed roughly at the same time in Figure 6. The maximum effect is -1.3°C, peaking around 7pm, with an average reduction of 0.5°C for more than 15 hours.

The presence of trees around the case station appears to have marginally increased relative humidity by +1.6% on average. Effects on relative humidity remain mostly within the margin of error of the test, with only minor significant effects lasting about 5 hours in total. These minor changes do not have a significant impact on pedestrian heat stress given how dry conditions are to start with. A strong decrease is observed around 9 am, although the reason for it is unclear. As both variables are dependent, in order to clarify the impact of the variation of T_a on relative humidity, absolute humidity AH (g/m^3) is plotted in Figure 8.

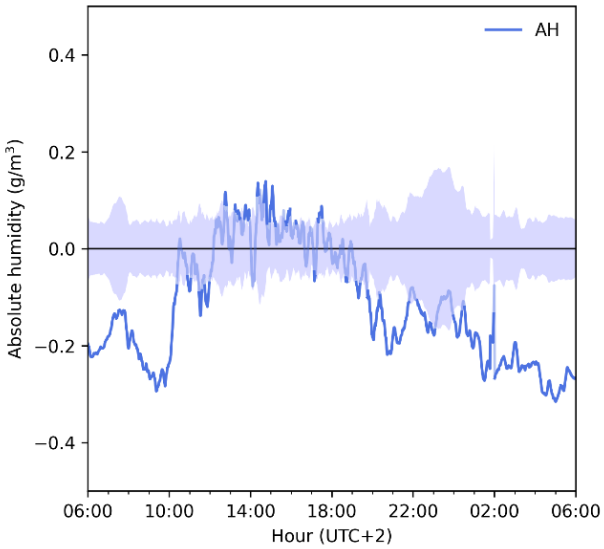

Figure 8: Average effects of the site's conversion on absolute humidity (AH).

AH seems to decrease in the morning and evening, while it increases in the afternoon, although these variations remain small. The maximum AH reduction is up to -0.3 g/m^3 with an average stat. sign. drop of -0.2 g/m^3 for about 16 hours. As it stands, given T_a and RH, this means that the drop

in air temperature is amplified by the decrease in absolute humidity. Since *AH* is likely to increase with future tree growth, this could counterbalance the drop in air temperature.

Figure 9 shows the average effects of the conversion on the radiative load (mean radiant temperature minus air temperature, $MRT - T_a$) and *UTCI*-equivalent temperature (note that results were found to be extremely similar between *MRT* and radiative load).

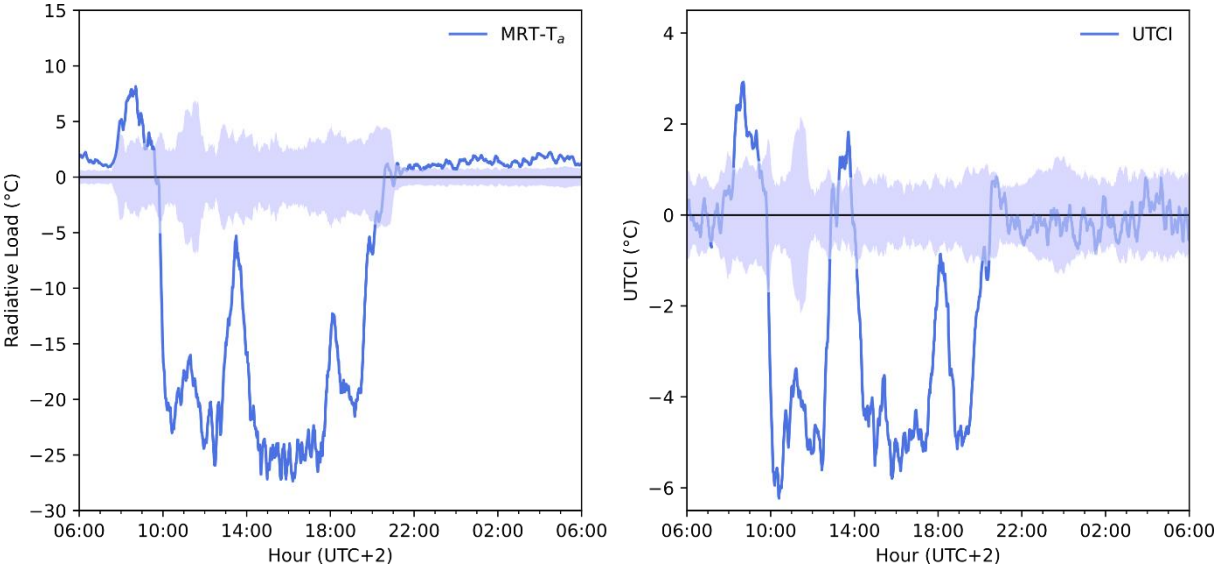

Figure 9: Average microclimatic effects of the site's conversion. ($MRT - T_a$): radiative load, (*UTCI*): *UTCI*-equivalent temperature.

For ($MRT - T_a$), three distinct major peaks of reduction are observed, respectively between 10 am to 12:30 pm, 2-5:30 pm and 6:30-8:00 pm. These are principally attributable to morning and afternoon shade, causing a very substantial maximum reduction in the radiative load of up to 27°C, for an average reduction of all stat. sign. effects of 8.2°C for more than 19 hours. The newly planted trees reduce *SVF* (from 0.7 to 0.2 here), thus strongly reducing the radiative load in daytime (Tan et al. 2016). In a simulation study on the effects of vegetation for Montreal, Wang & Akbari (2016) showed that planting vegetation with a reduction of *SVF* from 0.7 to 0.2 led to respective reductions at midday and midnight of air temperature up to 3.8°C and 2.2°C, and of *MRT* up to 36.5°C and 1.8°C. We find similar results here for daytime.

The shape and position of cooling peaks on ($MRT - T_a$) have direct repercussions on *UTCI*. The maximum *UTCI* reduction reaches -6.2°C at 10:30 am for an average reduction of -3.1°C during about 11 hours per day. At night, a marginal stat. sign. increase of up to 3°C ($MRT - T_a$) is observed, most likely because of the increase of incident infrared radiation *L* (see Figure 6) which is the only parameter likely to increase radiative load at that time given the results. This is found to be inconsequential on the average effect on *UTCI*, which, at night, oscillates around zero and remains within the margin of error of the test as early as 8:30 pm. Similarly, Milošević et al. (2017) reported simulated *UTCI* reductions of up to 3.3°C following the greening of a parking lot.

It is to be noted, however, that both the radiant load and *UTCI* increase briefly at the very start of insolation around 8 - 9 am by approximately 7° and 3°C, respectively. During that period, the amount of solar radiation reflected by the pavement has already increased due to the higher pavement albedo (0.24 vs 0.13), while incident solar radiation has not yet decreased (Figure 6). This suggests that the configuration of the site in the early morning is such that trees do not yet provide shade to the sensors, while the higher albedo of the ground is increasing mean radiant temperature *MRT*. As such, the situation is detrimental to pedestrians, although the effect is relatively weak and short in duration. Indeed, reflective pavements are identified in the literature as an *UHI*-mitigation strategy, but the effect on thermal comfort is unclear and remains understudied. Many studies

reported significant reductions of surface temperature, and sometimes air temperature in open urban spaces, all the more with low wind speeds (Santamouris 2013, Taleghani 2018). However, other studies have reported little effect or even increases of air temperature, while reporting significant increases of *MRT* and thus a deterioration of pedestrian thermal comfort (Taleghani 2018, Lopez-Cabeza 2022). These same studies recommend medium albedo for balancing positive and negative effects, and suggest vegetation as a better choice for limiting pedestrian heat stress.

Our results also show a minor deterioration of *UTCI* between 1- 1:30 pm as well. Although the radiative load ($MRT - T_a$) is reduced at that time, the signal rises slightly as does that of air temperature, which could possibly explain this observation.

○ Average Effects on Wind Speed

A histogram of wind speed and direction at the case station for all radiative days is shown in Figure 10. The statistical impact of the conversion on wind speed is shown in Figure 11 and summarized in Table 7. As can be seen, tree planting has modified the airflow pattern of the site, and a slight change of direction is exhibited. Wind speed is reduced up to 1.22 m/s, and by 0.65 m/s on average. However, wind speed reduction is found inconsequential on pedestrian heat stress (which is improved), as seen previously.

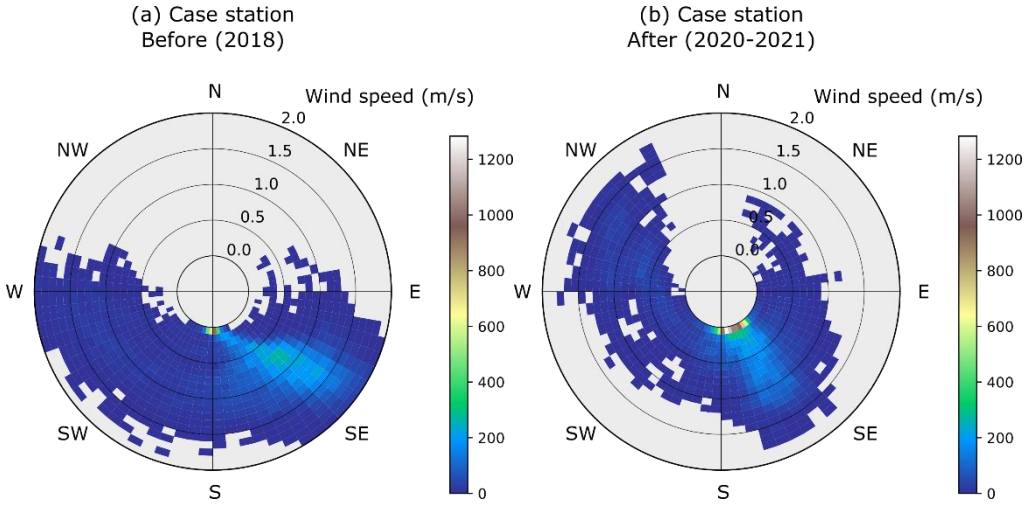

Figure 10: Histogram of case-station wind speed and direction. (a): Before conversion, (b): After conversion. All data (each minute) from each radiative day is used. The color bar is the occurrence based on a binning of 0.1 m/s for wind speed and 5° for wind direction.

Table 7: Mean, maximum and duration of the statistically significant effects on wind speed of the site's conversion at case station location, 24h-average effect and associated p-value if statistically significant.

	Wind speed
Average value of the stat. sign. events	-0.65 m/s
Duration of the stat. sign. events	14h
Maximum stat. sign. effect	-1.22 m/s
24h-averaged value	-0.46 m/s
p-value associated with the 24-h average if stat. sign	2.0e-4

Wind speed reductions consecutive to tree planting may be responsible for higher levels of air pollution (Arghavani et al. 2020), and may slow down cooling of the area, especially at night. Van Hove et al. (2015) showed that a wind speed reduction of 1 m/s lead to an increase in Physiological Equivalent Temperature (*PET)* of 9°C from fixed measurements in Rotterdam, all else being equal. Morakinyo et al. (2017) found that trees improved daytime thermal comfort in dense urban environments, but trapped infrared radiation and reduced wind circulation, which caused worsening of thermal comfort at night, especially in deep urban canyons. They recommend taller trees with low canopy density in deep urban canyons ($H/W>1$), and the opposite for open-areas

(H/W<1). It is noteworthy that wind speed could be tested for other weather conditions than radiative days to study the impact of trees on more wind patterns, although we did consider that for this paper.

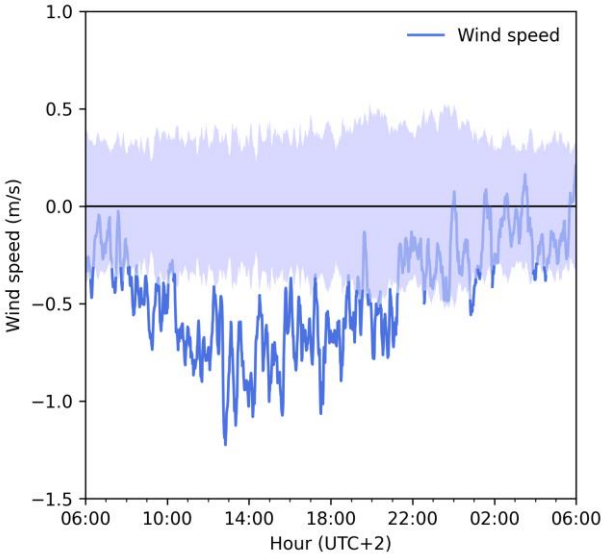

Figure 11: Average effects on wind speed of the site's conversion.

3.2. Mobile Microclimatic Measurements

We now present results of the microclimatic mobile measurements for characterizing heat stress at pedestrian height in several locations of the site, which could be less favorable to pedestrians than where the fixed case station for fixed measurements. Two mobile measurement campaigns are presented (before/after conversion). Figure 12 shows meteorological conditions measured at the control (rooftop) station during each mobile measurement campaign. Mobile measurements were carried out between 2:30pm and 5:30pm. The corresponding time window is highlighted in grey in Figure 12. Due to datalogger error, no data was recorded from 2am to 6am (day+1) during the second mobile campaign in 2021, though irrelevant here. Weather conditions were quite similar between mobile campaigns, though slightly hotter and more humid after conversion, and with less incident solar radiation. Differences in radiation tend to shrink in the afternoon, when measurements were performed.

The mobile measurement points within the site are shown in Figure 13a (point 2 is located near the fixed case weather station). Figure 13b and c respectively show thermal over-stress $\Delta UTCI$ (see eq. 2) at the six measurement points before and after renovation. Note that point 3 was not shaded by the adjacent building : it was in the sun in 2018 and in very sparse tree shade in 2021, since fewer trees were planted in this area. Point 4 was completely shaded by the building both in 2018 and 2021, and point 5 was in the sun for both campaigns.

Points 4 and 5 are located outside of the renovation area and can therefore be considered as reference points where no change in conditions is expected. Despite the lack of renovation in these two areas, we note that the value of $\Delta UTCI$ is not constant. Differences in weather conditions between campaigns could explain this (in particular for wind and radiation, which we use to select radiative days). Solar radiation was indeed lower post-renovation, as was MRT (Figure 12). However, we emphasize that differences in weather conditions between campaigns has a limited impact, since mobile measurements are analyzed relative to control measurements performed simultaneously (eq. 2). In principle, comparison pre- and post-states should be realistic as long as the control station remains unchanged and mobile measurements are performed during radiative days. Nonetheless, in reality local microclimatic fluctuations influence the thermal footprint of points 4 and 5 and of the control (despite our radiative day criteria). Overcoming this would

translate to switching to a statistical method averaging several radiative days pre- and post-conversion, i.e. as for the fixed measurements method presented in section 3.1. The fluctuation of Δ*UTCI* between campaigns for points 4 and 5 thus provides a rough estimate of the uncertainty associated with our mobile methodology, which is about 1 - 2°C. Results of Figure 13 within this range should thus be considered with reserve.

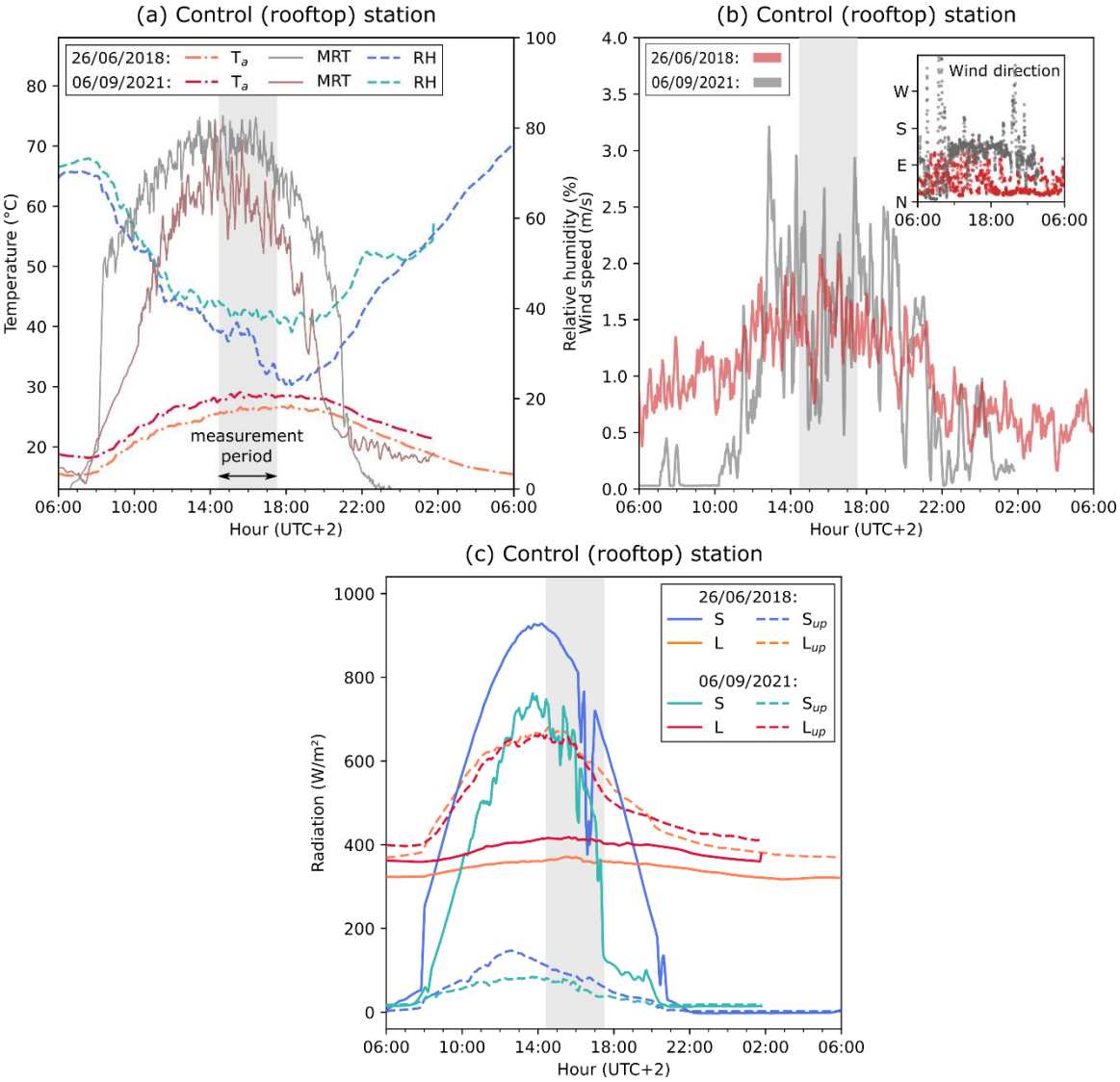

Figure 12: Weather conditions at fixed control (rooftop) station during mobile measurements (before conversion: 26/06/2018, after conversion: 06/09/2021). (a): air temperature (T_a), mean radiant temperature (MRT), and relative humidity (*RH*), (b): wind speed and wind prevalent direction, (c): incident and upwards solar radiation (resp. *S* and S_{up}), incident and upwards infrared radiation (resp. *L* and L_{up}).

At points 1, 2, and 3, the impact of the site's conversion is manifest: we observe that Δ*UTCI* decreases strongly between 2018 and 2021. The most important reduction is observed at point 2 for which Δ*UTCI* decreases by about 8°C after renovation. Yet, as can be seen in Figure 14 (close-up of weather data measured at the mobile points) wind speed was slightly lower in 2021, while the difference in air temperature with the control (rooftop) air temperature ($T_a - T_a^{control}$) was relatively similar between campaigns. This reduction in Δ*UTCI* is therefore mainly explained by a significant decrease in relative radiant load, as shown in Figure 14.

The reduction in thermal over-stress exhibited here at points 1, 2 and 3 is all the more significant as vegetation grew thicker and taller between 2020 (newly planted trees) and 2021 (post-renovation measurement campaign), as illustrated in Figure 15.

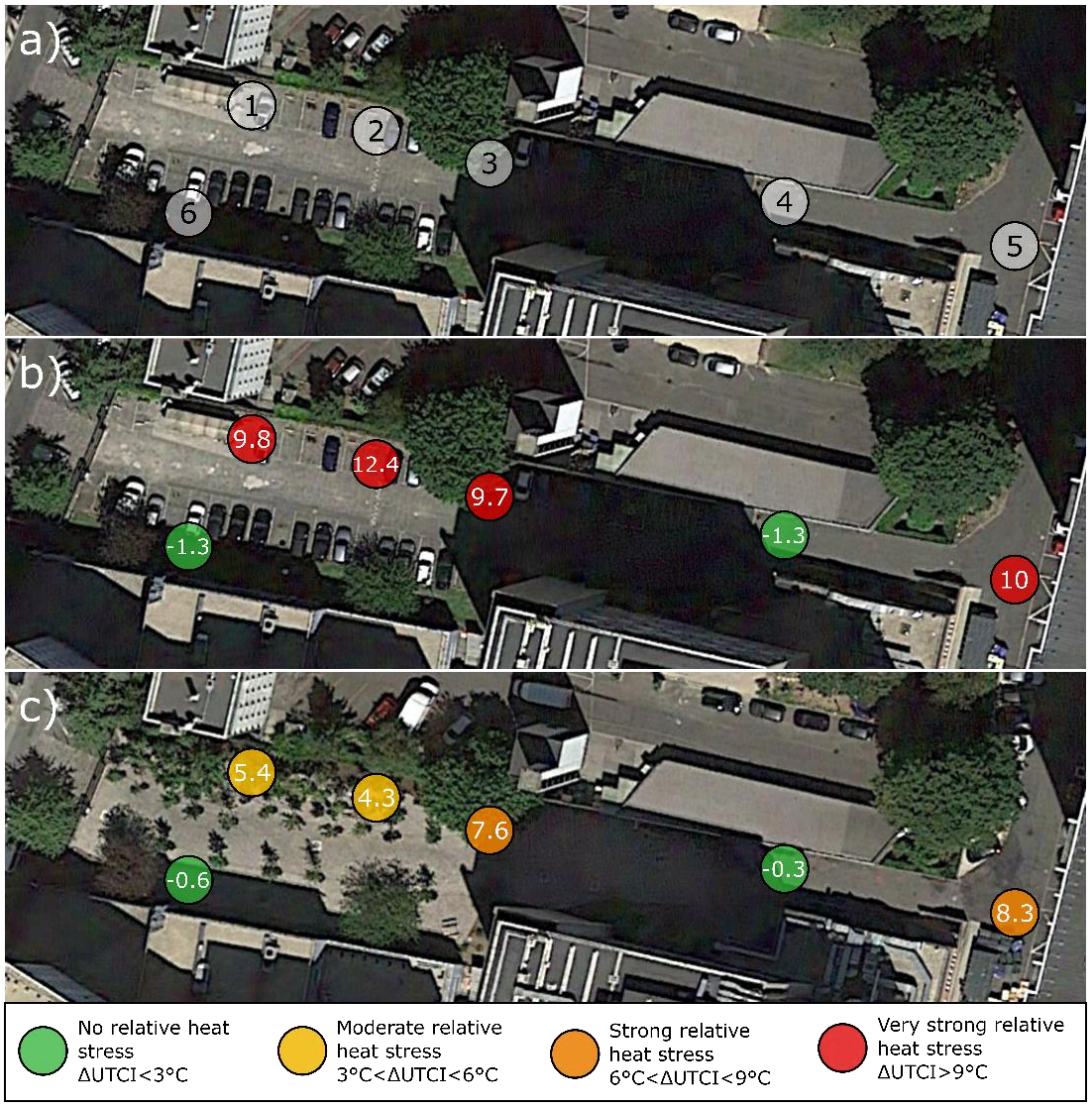

Figure 13: a) Measurement points, b) thermal over-stress before renovation (June 2018), c) thermal over-stress after renovation (September 2021).

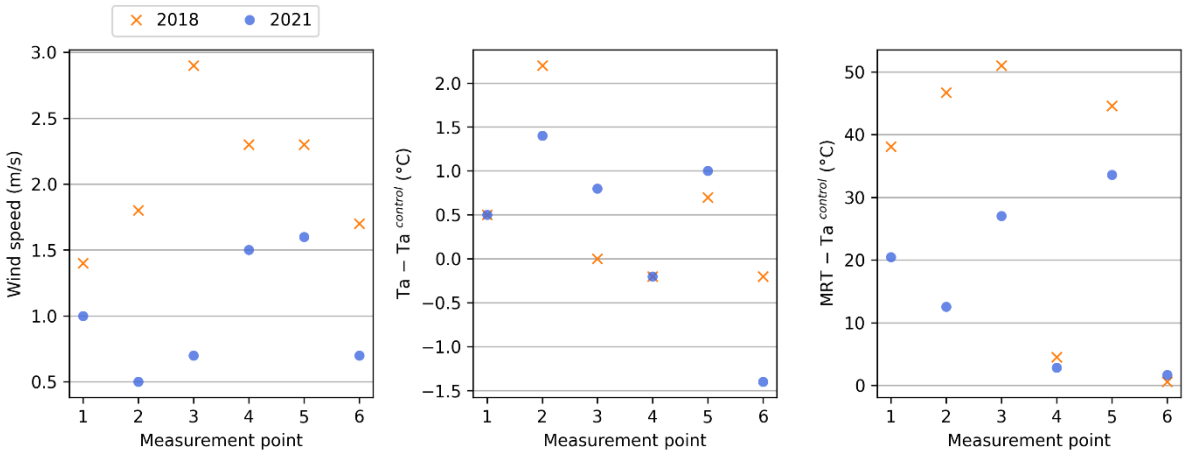

Figure 14: Mobile weather data for both mobile campaigns. Left to right: wind speed, air temperature difference with control air temperature ($T_a - T_a^{control}$) and relative radiant load ($MRT - T_a^{control}$).

The spatial cartography of the site shows that areas shaded by buildings, i.e. points 4 and 6, remain by far the most beneficial areas for pedestrians in terms of heat stress. These points offer almost no thermal over-stress with regard to the reference situation once the experimental protocol's uncertainty is accounted for. Similar results were found by Sashua-Bar et al. (2011) comparing tree-shade and directly exposed areas.

Points 1 and 2 (and to a lesser extent point 3) exhibit moderate relative heat stress (with regard to the reference *UTCI*), which, as already discussed in the paragraph above, was greatly reduced following the conversion of site. Compared with points 4 and 6, these points exhibit sparser shade compared to buildings as the trees are still young. In addition, the northern side of the site (where points 1 and 2 are located) was specifically densely vegetated because of its naturally higher exposure to the sun, hence conditions are harsher to begin with in this area. Thermal stress at points 1, 2 (and 3) is likely to decrease with tree growth in the future, while that of points 4 and 6 should remain globally unchanged.

In contrast, the least favorable areas for a pedestrian are point 5, followed by point 3, which both offer very strong to strong heat over-stress after conversion. Indeed, point 5 (not transformed) is under the sun and presents a dark impervious asphalt pavement. For its part, although point 3 is located within the renovation area with permeable concrete, it is located in a sparsely planted area and is in the sun most of the time. Point 3 shows a weak improvement of thermal stress between 2018 and 2021, considering the uncertainty of the method. This suggests that the effect of the permeable concrete (with an albedo of 0.24 vs 0.13 for the old asphalt concrete) on heat stress, if existent, remains very limited (whether beneficial or detrimental) contrary to the impact of shade that is quite clear (points 1 and 2). Fixed station measurements corroborate this, showing that the increase in S_{up} is more or less compensated by the decrease in L_{up} near point 2. This observation for point 3 is not sufficient to determine the cause of the deterioration of heat stress in the early morning observed in Figure 9 with the fixed station, which we suspect could be caused by the higher albedo of concrete. This therefore still needs additional investigations to conclude.

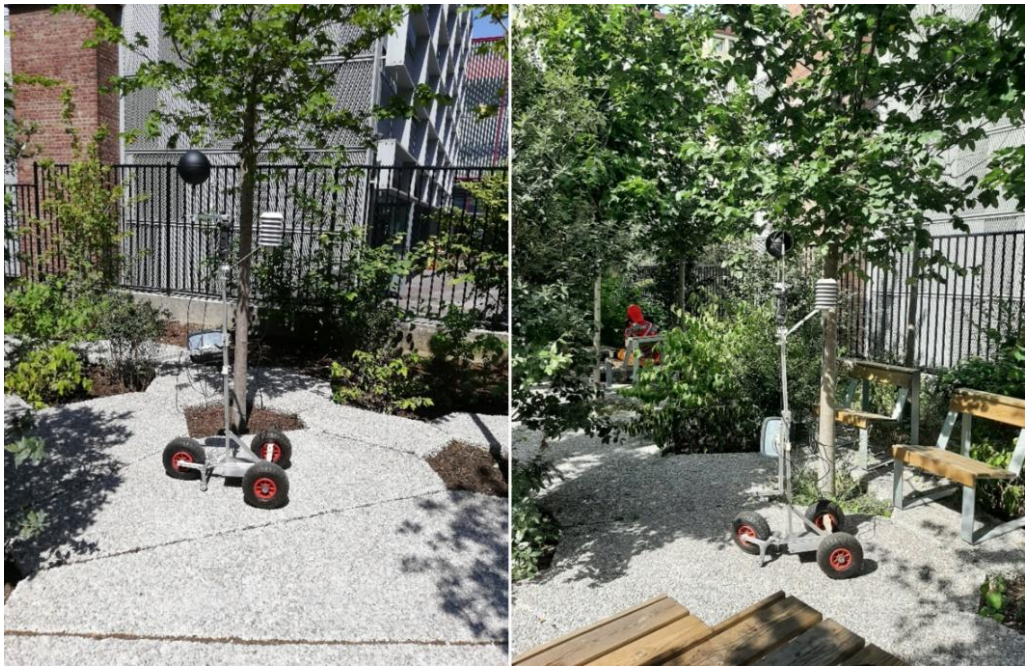

Figure 15: Mobile weather station at point 1 in 2020 (left) and in 2021 (right).

Our results confirm how exposition to direct solar radiation is critical for pedestrian heat stress (Xiong & He 2022, Xie et al. 2022). It is noteworthy that even small changes in heat stress after conversion can still be pleasurable for pedestrians (Dzyuban et al. 2022).

4. Conclusion and Recommendations

The effects on microclimate of the conversion of a parking lot into a small urban forest with 72 trees and permeable concrete were determined. We proposed a monitoring protocol combining fixed and mobile measurements during summer in order to, respectively, estimate robust statistical effects over 24h constructed with several days of observation, and compare spatial distribution of heat stress pre- and post-conversion, both regardless of differences in weather conditions. Future tree growth will likely increase shade and hence all of the observed microclimatic effects summarized hereafter.

Where trees were densely planted, extremely statistically robust effects were exhibited, both in amplitude and duration. Underneath the trees, solar radiation and upwards infrared radiation decrease, while upwards solar radiation and incident infrared radiation increase slightly, following the creation of shade and the higher pavement albedo (reduced SVF and reduced pavement temperature). Accounting for all above radiative components, the radiative load on the pedestrian is thus significantly reduced (by -175 W/m² on a 24h average, and up to -490 W/m² at most).

The newly designed area also exhibited reductions in air temperature, radiative load ($MRT - T_a$), wind speed and slight increase of relative humidity. Despite negative effects on RH and wind speed, other effects on radiation and microclimate translated into a strong and durable benefit for heat stress ($UTCI$) at pedestrian height, by -3.1°C on a 24h average, and up to -6.2°C. Effects on $UTCI$ are very substantial during the day, though practically non-existent at night, contrary to most of the other parameters.

The spatial characterization of heat stress on the site showed that thermal over-stress is strongly reduced where the most trees were planted (-8°C between campaigns) due to a reduction of the radiative load as a result of shading. Shade from newly planted trees offered the second most beneficial spot for pedestrians, despite the surroundings being highly exposed to the sun, while the most pleasurable spots are located near circling buildings, which almost permanently provide substantial shade compared to that provided by young trees. Unsurprisingly, unpleasant areas are those directly exposed to the sun, with little perceived difference between pavements (asphalt concrete versus permeable concrete).

While fixed monitoring has sufficient data to ensure a certain degree of statistical robustness, small differences in mobile measurements before and after conversion should be considered with caution. Further mobile campaigns are necessary to address the lack of hindsight associated with the proposed mobile measurement methodology.

Our findings can be useful to urban planners who seek guidelines for designing green urban areas for heat mitigation. Results confirm previous research that urban greening has an extremely positive impact on pedestrian thermal comfort, especially during the day when heat stress is the highest. The best areas for greening are thus highly open and exposed ones. For open urban settings, planting trees with a high density in areas directly exposed to sunlight to provide extensive shading is recommended in order to improve effectiveness on heat stress. This is particularly important given that the range of the shading effects is spatially limited. Finally, to ensure that pedestrians benefit most from the design, the area underneath the trees should be made accessible and attractive, for instance with sitting amenities.

Our findings also showed some negative effects, such as wind speed reduction and an increase of infrared radiative trapping at night due to the reduction of the sky view factor. For now, this is inconsequential on heat stress, but radiative cooling could further reduce with tree growth, as could convective cooling due to the decrease of wind circulation. For this reason, for denser, more compact areas (urban canyons, narrow streets etc.), we recommend meticulous planning and sparser tree planting, to avoid accumulated infrared trapping during nighttime, where wind circulation is already limited due to the urban configuration. This could worsen thermal comfort.

For such configurations, removable shading devices could be used daytime and removed nighttime to maximize radiative cooling and wind circulation.

Building shade was also found to be beneficial for pedestrians, though less attractive than greenery. Clever urban design should take advantage of existing shade and consider pedestrians' behavioral patterns to enhance and propose pleasant paths combining several solutions (building shade, trees, removable artificial shade). It is however noteworthy that trees provide multiple other benefits and should be privileged when possible. Care should be given to water availability. Pervious materials with underground rainwater storage systems – as is the case in this urban project – serve this need.

Finally, our results tend to indicate a negative effect of the higher-albedo concrete in the morning before the fixed station is shaded by the trees with a brief increase in heat stress of 3°C *UTCI*. Reflective pavements should preferentially target open areas with high sky view factors to avoid radiative trapping. Effect of low *SVF* on air pollution was not studied in this paper but could be interesting future work.

Acknowledgements

The authors acknowledge the financial and in-kind contributions of the Urban Materials for Cool Cities (UMat4CC) project funded by the French National Research Agency (ANR-18-CE22-0015-01), Alteralia, the French Environment & Energy Management Agency, the Paris Climate Agency and LafargeHolcim to this project.

References

Abdi, B., Hami, A., & Zarehaghi, D. (2020). Impact of small-scale tree planting patterns on outdoor cooling and thermal comfort. *Sustainable Cities and Society*, *56*, 102085.

Akbari, H, M Pomerantz, and H Taha. 2001. "Cool Surfaces and Shade Trees to Reduce Energy Use and Improve Air Quality in Urban Areas." Solar Energy 70 (3): 295–310. https://doi.org/10.1016/S0038-092X(00)00089-X.

Arghavani, S., Malakooti, H., & Bidokhti, A. (2020). Numerical assessment of the urban green space scenarios on urban heat island and thermal comfort level in Tehran Metropolis. Journal of cleaner production, 261, 121183.

ASTM E1918-16, "Standard Test Method for Measuring Solar Reflectance of Horizontal and Low-Sloped Surfaces in the Field," *ASTM International*, vol. i. West Conshohocken, PA, pp. 18–20, 2016.

Azcarate, I., Acero, J. A., Garmendia, L., & Rojí, E. (2021). Tree layout methodology for shading pedestrian zones: Thermal comfort study in Bilbao (Northern Iberian Peninsula). *Sustainable Cities and Society*, *72*, 102996.

Bouzouidja, R., Cannavo, P., Bodénan, P., Gulyás, Á., Kiss, M., Kovács, A., ... & Rodriguez, F. (2021). How to evaluate nature-based solutions performance for microclimate, water and soil management issues–Available tools and methods from Nature4Cities European project results. *Ecological Indicators*, *125*, 107556.

Bouzouidja, R., Leconte, F., Kiss, M., Pierret, M., Pruvot, C., Détriché, S., ... & Pétrissans, M. (2021). Experimental Comparative Study between Conventional and Green Parking Lots: Analysis of Subsurface Thermal Behavior under Warm and Dry Summer Conditions. *Atmosphere*, *12*(8), 994.

Bowler, Diana E., Lisette Buyung-Ali, Teri M. Knight, and Andrew S. Pullin. 2010. "Urban Greening to Cool Towns and Cities: A Systematic Review of the Empirical Evidence." *Landscape and Urban Planning* 97 (3): 147–55. https://doi.org/10.1016/j.landurbplan.2010.05.006.

Coccolo, S., Pearlmutter, D., Kaempf, J., & Scartezzini, J. L. (2018). Thermal Comfort Maps to

estimate the impact of urban greening on the outdoor human comfort. *Urban forestry & urban greening*, *35*, 91-105.

Das, M., Das, A., & Momin, S. (2022). Quantifying the cooling effect of urban green space: A case from urban parks in a tropical mega metropolitan area (India). *Sustainable Cities and Society*, *87*, 104062.

Dzyuban, Y., Hondula, D. M., Vanos, J. K., Middel, A., Coseo, P. J., Kuras, E. R., & Redman, C. L. (2022). Evidence of alliesthesia during a neighborhood thermal walk in a hot and dry city. *Science of the Total Environment*, *834*, 155294.

Fiala, D., Havenith, G., Bröde, P., Kampmann, B., & Jendritzky, G. (2012). UTCI-Fiala multi-node model of human heat transfer and temperature regulation. *International journal of biometeorology*, *56*(3), 429-441.

Fieldwork Architecture. (2023). Project "Tertiary Forest" website (in French): https://www.tierceforet.com/ (last accessed in June 2023).

Fu, J., Dupre, K., Tavares, S., King, D., & Banhalmi-Zakar, Z. (2022). Optimized greenery configuration to mitigate urban heat: A decade systematic review. Frontiers of Architectural Research.

Garschagen, M., & Romero-Lankao, P. (2015). Exploring the relationships between urbanization trends and climate change vulnerability. *Climatic Change*, *133*, 37-52.

Hendel, M., Gutierrez, P., Colombert, M., Diab, Y., & Royon, L. (2016). Measuring the effects of urban heat island mitigation techniques in the field: Application to the case of pavement-watering in Paris. *Urban Climate*, *16*, 43-58.

Hendel, M., Bobée, C., Karam, G., Parison, S., Berthe, A., & Bordin, P. (2020). Developing a GIS tool for emergency urban cooling in case of heat-waves. *Urban Climate*, *33*, 100646.

Hiemstra, J. A., Saaroni, H., & Amorim, J. H. (2017). The urban heat Island: Thermal comfort and the role of urban greening. In The Urban Forest (pp. 7-19). Springer, Cham.

IPCC, 2019: Summary for Policymakers. In: Climate Change and Land: an IPCC special report on climate change, desertification, land degradation, sustainable land management, food security, and greenhouse gas fluxes in terrestrial ecosystems [P.R. Shukla, J. Skea, E. Calvo Buendia, V. Masson-Delmotte, H.- O. Pörtner, D. C. Roberts, P. Zhai, R. Slade, S. Connors, R. van Diemen, M. Ferrat, E. Haughey, S. Luz, S. Neogi, M. Pathak, J. Petzold, J. Portugal Pereira, P. Vyas, E. Huntley, K. Kissick, M. Belkacemi, J. Malley, (eds.)]. https://doi.org/10.1017/9781009157988.001

Jia, S., & Wang, Y. (2021). Effect of heat mitigation strategies on thermal environment, thermal comfort, and walkability: A case study in Hong Kong. *Building and Environment*, *201*, 107988.

Karam, G., Chanial, M., Hendel, H., & Royon, L. (2022). Spatial Microclimatic Characterization of a Parisian "Oasis" Schoolyard. 5th International Conference on Building Energy and Environment, COBEE, 25th-29th July 2022, Montreal, Canada.

Kong, L., Lau, K. K. L., Yuan, C., Chen, Y., Xu, Y., Ren, C., & Ng, E. (2017). Regulation of outdoor thermal comfort by trees in Hong Kong. Sustainable Cities and Society, 31, 12-25.

Kousis, I., Manni, M., & Pisello, A. L. (2022). Environmental mobile monitoring of urban microclimates: A review. *Renewable and Sustainable Energy Reviews*, *169*, 112847.

Leconte, F., Bouyer, J., Claverie, R., & Pétrissans, M. (2015). Using Local Climate Zone scheme for UHI assessment: Evaluation of the method using mobile measurements. Building and Environment, 83, 39-49.

Li, J., Liu, Q., & Sang, Y. (2012). Several issues about urbanization and urban safety. *Procedia engineering*, *43*, 615-621.

Li, Y., Hong, B., Wang, Y., Bai, H., & Chen, H. (2022). Assessing heat stress relief measures to enhance outdoor thermal comfort: A field study in China's cold region. *Sustainable Cities and*

Society, *80*, 103813.

Lopez-Cabeza, V. P., Alzate-Gaviria, S., Diz-Mellado, E., Rivera-Gomez, C., & Galan-Marin, C. (2022). Albedo influence on the microclimate and thermal comfort of courtyards under Mediterranean hot summer climate conditions. Sustainable Cities and Society, 81, 103872.

Mahmoud, R. M. A., & Abdallah, A. S. H. (2022). Assessment of outdoor shading strategies to improve outdoor thermal comfort in school courtyards in hot and arid climates. *Sustainable Cities and Society*, *86*, 104147.

Milošević, D. D., Bajšanski, I. V., & Savić, S. M. (2017). Influence of changing trees locations on thermal comfort on street parking lot and footways. Urban forestry & urban greening, 23, 113-124.

Mitchell, D., Heaviside, C., Vardoulakis, S., Huntingford, C., Masato, G., Guillod, B. P., ... & Allen, M. (2016). Attributing human mortality during extreme heat waves to anthropogenic climate change. *Environmental Research Letters*, *11*(7), 074006.

Morakinyo, T. E., Kong, L., Lau, K. K. L., Yuan, C., & Ng, E. (2017). A study on the impact of shadow-cast and tree species on in-canyon and neighborhood's thermal comfort. Building and Environment, 115, 1-17.

Nwakaire, C. M., Onn, C. C., Yap, S. P., Yuen, C. W., & Onodagu, P. D. (2020). Urban Heat Island Studies with emphasis on urban pavements: A review. *Sustainable Cities and Society*, *63*, 102476.

Oke, T. R. (1982). The energetic basis of the urban heat island. *Quarterly journal of the royal meteorological society*, *108*(455), 1-24.

Parece, T. E., Li, J., Campbell, J. B., & Carroll, D. (2016). Assessing urban landscape variables' contributions to microclimates. Advances in Meteorology, 2016.

Parison, S., Hendel, M., Grados, A., & Royon, L. (2020a). Analysis of the heat budget of standard, cool and watered pavements under lab heat-wave conditions. *Energy and Buildings*, *228*, 110455.

Parison, S., Hendel, M., & Royon, L. (2020b). A statistical method for quantifying the field effects of urban heat island mitigation techniques. Urban Climate, 33, 100651. https://doi.org/10.1016/j.uclim.2020.100651

Parison, S., Hendel, M., Grados, A., Jurski, K., & Royon, L. (2021). A radiative technique for measuring the thermal properties of road and urban materials. *Road Materials and Pavement Design*, *22*(5), 1078-1092.

Pena, J. C. D. C., Martello, F., Ribeiro, M. C., Armitage, R. A., Young, R. J., & Rodrigues, M. (2017). Street trees reduce the negative effects of urbanization on birds. *PloS one*, *12*(3), e0174484.

Peng, Z., Bardhan, R., Ellard, C., & Steemers, K. (2022). Urban climate walk: A stop-and-go assessment of the dynamic thermal sensation and perception in two waterfront districts in Rome, Italy. *Building and Environment*, *221*, 109267.

Pigliautile, I., & Pisello, A. L. (2018). A new wearable monitoring system for investigating pedestrians' environmental conditions: Development of the experimental tool and start-up findings. Science of the total environment, 630, 690-706.

Qi, Q., Meng, Q., Wang, J., & Ren, P. (2021). Developing an optimized method for the 'stop-and-go' strategy in mobile measurements for characterizing outdoor thermal environments. Sustainable Cities and Society, 69, 102837.

Qi, Q., Meng, Q., Wang, J., He, B., Liang, H., & Ren, P. (2022). Applicability of mobile-measurement strategies to different periods: A field campaign in a precinct with a block park. Building and Environment, 108762.

Raman, V., Kumar, M., Sharma, A., & Matzarakis, A. (2021a). A quantitative assessment of the dependence of outdoor thermal-stresses on tree-building morphology and wind: A case-study in sub-tropical Patna, India. *Sustainable Cities and Society*, *73*, 103085.

Raman, V., Kumar, M., Sharma, A., Froehlich, D., & Matzarakis, A. (2021b). Quantification of thermal stress abatement by trees, its dependence on morphology and wind: A case study at Patna, Bihar, India. *Urban Forestry & Urban Greening*, *63*, 127213.

Santamouris, M. (2013). Using cool pavements as a mitigation strategy to fight urban heat island—A review of the actual developments. Renewable and Sustainable Energy Reviews, 26, 224-240.

Santamouris, M., Cartalis, C., Synnefa, A., & Kolokotsa, D. (2015). On the impact of urban heat island and global warming on the power demand and electricity consumption of buildings—A review. *Energy and buildings*, *98*, 119-124.

Santamouris, M. (2015). Regulating the damaged thermostat of the cities—Status, impacts and mitigation challenges. *Energy and Buildings*, *91*, 43-56.

Setälä, H., Viippola, V., Rantalainen, A. L., Pennanen, A., & Yli-Pelkonen, V. (2013). Does urban vegetation mitigate air pollution in northern conditions?. *Environmental pollution*, *183*, 104-112.

Shashua-Bar, L., Pearlmutter, D., & Erell, E. (2011). The influence of trees and grass on outdoor thermal comfort in a hot-arid environment. International journal of climatology, 31(10), 1498-1506.

Sheets, V. L., & Manzer, C. D. (1991). Affect, cognition, and urban vegetation: Some effects of adding trees along city streets. *Environment and Behavior*, *23*(3), 285-304.

Shi, Y., Lau, K. K. L., Ren, C., & Ng, E. (2018). Evaluating the local climate zone classification in high-density heterogeneous urban environment using mobile measurement. Urban Climate, 25, 167-186.

Shuaib, M., Ali, K., Ahmed, S., Hussain, F., Ilyas, M., Hassan, N., ... & Hussain, F. (2018). Impact of rapid urbanization on the floral diversity and agriculture land of district Dir, Pakistan. *Acta Ecologica Sinica*, *38*(6), 394-400.

Stewart-Oaten, A., Murdoch, W. W., & Parker, K. R. (1986). Environmental impact assessment:" Pseudoreplication" in time?. Ecology, 67(4), 929-940.

Stewart, I. D., & Oke, T. R. (2012). Local climate zones for urban temperature studies. Bulletin of the American Meteorological Society, 93(12), 1879-1900.

Sulzer, M., Christen, A., & Matzarakis, A. (2022). A Low-Cost Sensor Network for Real-Time Thermal Stress Monitoring and Communication in Occupational Contexts. Sensors, 22(5), 1828.

Takebayashi, H., & Moriyama, M. (2009). Study on the urban heat island mitigation effect achieved by converting to grass-covered parking. Solar Energy, 83(8), 1211-1223.

Taleghani, M. (2018). Outdoor thermal comfort by different heat mitigation strategies-A review. Renewable and Sustainable Energy Reviews, 81, 2011-2018.

Tan, Z., Lau, K. K. L., & Ng, E. (2016). Urban tree design approaches for mitigating daytime urban heat island effects in a high-density urban environment. Energy and Buildings, 114, 265-274.

Teshnehdel, S., Akbari, H., Di Giuseppe, E., & Brown, R. D. (2020). Effect of tree cover and tree species on microclimate and pedestrian comfort in a residential district in Iran. *Building and Environment*, *178*, 106899.

Uttara, S., Bhuvandas, N., & Aggarwal, V. (2012). Impacts of urbanization on environment. *International Journal of Research in Engineering and Applied Sciences*, *2*(2), 1637-1645.

Van Hove, L. W. A., Jacobs, C. M. J., Heusinkveld, B. G., Elbers, J. A., Van Driel, B. L., & Holtslag, A. A. M. (2015). Temporal and spatial variability of urban heat island and thermal comfort within the Rotterdam agglomeration. Building and Environment, 83, 91-103.

Vardoulakis, S., & Kinney, P. (2019). Grand challenges in sustainable cities and health. *Frontiers in Sustainable Cities*, *1*, 7.

Vasilikou, C., & Nikolopoulou, M. (2020). Outdoor thermal comfort for pedestrians in movement: thermal walks in complex urban morphology. *International journal of biometeorology*, *64*, 277-291.

Wang, Y., & Akbari, H. (2016). The effects of street tree planting on Urban Heat Island mitigation in Montreal. Sustainable Cities and Society, 27, 122-128.

Xie, Y., Wang, X., Wen, J., Geng, Y., Yan, L., Liu, S., ... & Lin, B. (2022). Experimental study and theoretical discussion of dynamic outdoor thermal comfort in walking spaces: Effect of short-term thermal history. *Building and Environment*, *216*, 109039.

Xiong, K., Yang, Z., & He, B. J. (2022). Spatiotemporal heterogeneity of street thermal environments and development of an optimised method to improve field measurement accuracy. *Urban Climate*, *42*, 101121.

Xiong, K., & He, B. J. (2022). Wintertime outdoor thermal sensations and comfort in cold-humid environments of Chongqing China. *Sustainable Cities and Society*, *87*, 104203.

Zheng, X., Kong, F., Yin, H., Middel, A., Liu, H., Wang, D., ... & Lensky, I. (2021). Outdoor thermal performance of green roofs across multiple time scales: A case study in subtropical China. *Sustainable Cities and Society*, *70*, 102909.